Robot-Assisted Real-Time Tumor Manipulation for Breast Biopsy

Vishnu G. Mallapragada, Nilanjan Sarkar, *Senior Member, IEEE*, and Tarun K. Podder, *Member, IEEE*

***Abstract*—Breast biopsy guided by imaging techniques such as ultrasound is widely used to evaluate suspicious masses within the breast. The current procedure allows the clinician to determine the location and extent of a tumor in the patient breast before inserting the needle. However, there are several problems with this procedure: the complex interaction dynamics between the needle force and the breast tissue will likely displace the tumor from its original position, necessitating multiple insertions, causing clinicians' fatigue, patient's discomfort, and compromising the integrity of the tissue specimen. In this paper, we present a new concept for real-time manipulation of a tumor using a robotic controller that monitors the image of the tumor to generate appropriate external force to position the tumor at a desired location. The idea here is to demonstrate that it is possible to manipulate a tumor in real time by applying controlled external force in an automated way such that the tumor does not deviate from the path of the needle. Experiments on breast phantoms are presented to demonstrate the essence of this concept. The success of this approach has the potential to reduce the number of attempts a clinician makes to capture the desired tissue specimen, minimize tissue damage, improve speed of biopsy, reduce patient discomfort, and eliminate false negative results.**

***Index Terms*—Needle insertion, position control, robot-assisted biopsy, tumor manipulation.**

I. Introduction

BREAST cancer is the most common cancer among American women and the second leading cause of cancer death in women. In 2008, the American Cancer Society (ACS) estimates 182 460 (26% of all female malignancies) new breast cancer cases with 22% mortality rate [1]. Early detection of breast cancer has been proven to reduce mortality by about 20%–35% [2]. Histopathological examination is considered to be the "gold standard" for definitive diagnosis of cancer, but requires tissue samples that are collected through biopsy. Of the two major approaches for breast biopsy, needle biopsy and open excisional biopsy, needle biopsy is more attractive because it is less traumatic, produces little or no scar, allows quicker recovery, and is less costly. Despite many benefits of needle biopsy, there are significant technical challenges concerning accurate steering and precise placement of a biopsy needle at the target (in this paper, the word target is used to refer to a tumor, lesion, or just a suspected region of tissue) in the breast. To successfully remove a suspicious small targeted lump, various issues must be addressed, such as architectural distortion and target deflection during needle insertion and poor maneuverability of the biopsy needle. Currently, core samples are collected using large needles such as a 14-gauge (2.1 mm in diameter) true cutting needle, a 10-gauge (3.4 mm in diameter) vacuum-assisted needle, and other RF cutting instruments (En-bloc and Rubicor). Despite advances in needle technology, accurate placement of a biopsy needle at the target location remains a challenging task.

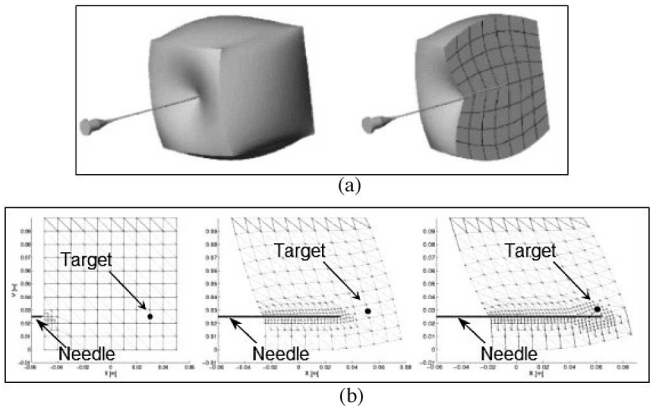

Fig. 1. Finite-element model of needle insertion in soft tissue [3]. (a) Cross section of 3-D model shows the finite-element mesh. (b) Target movement during needle insertion.

There are two major problems to be addressed to improve the accuracy and reduce the difficulty of obtaining tissue samples during needle biopsies.

1) *Target mobility*: During needle insertion, the complex tissue of the breast induces the small target to deflect away from its original location. Fig. 1 [3] shows a 3-D finite-element model of needle insertion that estimates the force distribution along the needle shaft. We can see from Fig. 1 that as the needle is inserted, large tissue deformation causes the target to move away from the line of insertion of the needle. This necessitates multiple insertions at the same biopsy site to successfully sample the target tissue.
2) *Difficulty of operation*: Needle biopsies are guided by stereotactic mammography, MRI, or 2-D ultrasound (US). Sonography is the widely used imaging technique

Manuscript received May 20, 2008; revised November 10, 2008 and December 3, 2008. First published February 20, 2009; current version published April 3, 2009. This paper was recommended for publication by Associate Editor F. Park and Editor C. Cavusoglu upon evaluation of the reviewers' comments. This paper was presented in part at the IEEE International Conference on Bioinformatics and Bioengineering, Boston, MA, October 14–17, 2007, and in part at the IEEE International Conference on Robotics and Automation, Pasadena, CA, May 19–23, 2008.

V. G. Mallapragada is with the Mechanical Engineering Department, Vanderbilt University, Nashville, TN 37212 USA (e-mail: vishnu.g.mallapragada@vanderbilt.edu).

N. Sarkar is with the Mechanical Engineering Department and the Computer Engineering Department, Vanderbilt University, Nashville, TN 37212 USA (e-mail: nilanjan.sarkar@vanderbilt.edu).

T. K. Podder is with the Department of Radiation Oncology, Thomas Jefferson University Hospital, Philadelphia, PA 19107 USA (e-mail: tarun.podder@jeffersonhospital.org).

Digital Object Identifier 10.1109/TRO.2008.2011418

because of its real-time capability and cost-effectiveness [4]. The current state-of-the-art US-guided biopsy technique is highly dependent on the skill of the clinician [5]. A clinician performs this procedure by holding the US probe with one hand and inserting the needle with the other. Since sonography provides only a 2-D image, if the target moves out of plane of the transducer, the clinician has to continuously reorient the probe to keep the needle and the target in the imaging plane while inserting the needle. It is critical to orient the imaging plane parallel to the needle; otherwise, a false impression of the needle tip causes sampling errors [6]. This freehand biopsy procedure requires excellent hand–eye coordination. Since stabilization of the breast is problematic [7] and steering of the needle inside the breast is extremely difficult, many insertion attempts are required to successfully sample the target tissue. This procedure is very fatiguing for the clinician and uncomfortable for the patient.

As can be seen from the earlier discussion, a robot-assisted breast biopsy system can help the clinician and address the aforementioned problems by: 1) providing a mechanism that stabilizes the breast and allows the needle to access the target considering target movement and 2) developing an automated image acquisition system that can be coupled with the needle insertion procedure. We are currently working on developing such a robot-assisted breast biopsy system. Our initial concepts and results were presented in [8] and [9]. This paper expands on this approach to control the target location in the breast such that the needle can be placed at the target location easily and quickly, thus reducing many of the disadvantages of the current needle biopsy procedure as described before. This control approach is developed in such a manner that it can be coupled with an automatic image acquisition system, the work that is currently underway.

The rest of the paper is organized as follows. Section II presents a review of the relevant literature. Section III casts the target positioning problem in a control framework and describes the overall architecture of the guiding mechanism. Section IV presents experimental results on a phantom. Section V summarizes the conclusions of this paper.

II. Literature Review

In this section, we review the literature related to needle biopsies of breast and discuss where our study stands in relation to the current state of the art. Commercially available biopsy instruments such as Bard Biopty-cut, Mammotome, and Advanced Breast Biopsy Instrumentation (ABBI) systems do not compensate for target movement during needle insertion.

Several groups have designed robotic systems to improve the accuracy of needle insertions [10]–[15]. The reader is referred to [10] for a detailed review of the state of the art in interventional robotic systems. Several systems such as a device for conditioning of the breast and positioning of the biopsy probe [11], robotic systems for needle insertion [12], precise intratumoral placement of therapeutic agents [13], and spinal [14] and renal [15] percutaneous procedures have been developed. "Although these innovations greatly improve accuracy by automating needle target alignment, they do not provide active trajectory correction in the likely event that trajectory errors arise" [16]. Needle trajectory errors and target mobility result in multiple insertions at the same biopsy site for accurate sampling. In addition, such sampling errors may increase false negative results.

As a result, significant research effort is being made to investigate techniques that can address the problem of target movement during needle insertion. Steerable devices are presented in [16]–[19] that allow the clinician to steer the tip of the needle toward the target during insertion. With such a device, the clinician would have to maneuver the needle using one hand with image data from a US monitor, while at the same time correctly orienting the US probe and stabilizing the breast with the other hand. As mentioned earlier, such a freehand biopsy technique is extremely difficult and fatiguing for the clinician and uncomfortable for the patient. A visually controlled needle-guiding system is developed in [20] for automatic or remote-controlled percutaneous interventions. In the automated mode, the needle insertion path is updated based on image feedback to the needle-guiding system. Though these systems potentially reduce the number of insertions required to sample the target, maneuvering a needle inside the breast causes tissue damage. A finite-element model of the breast is used in [21] and [22] to predict the movement of the target. The needle path is planned based on this prediction to accurately sample the target. To get an accurate prediction of the movement of the target, finite-element analysis requires the geometric model and mechanical properties of the breast. The average time for computation is 29 min in [21].

We take a diametrically opposite approach to this problem, i.e., instead of steering the needle toward the target during insertion, we guide the target toward the line of insertion of the needle. Our approach is to design an external robotic system that will be able to position the target in-line with the needle during insertion. The real-time target manipulation system presented here is a set of position-controlled actuators. These actuators are placed around the breast during the needle insertion procedure. They control the position of the target by applying forces on the surface of the breast such that the target is placed in-line with the needle. We demonstrate the success of this approach by casting this problem in a control framework. The idea is to design a controller that minimizes the tracking error in the position of the target. In this approach, needle insertion force is treated as a disturbance to the system.

III. Control Framework

During image-guided breast biopsy, a clinician inserts the needle through an incision to remove a tissue sample. A schematic of needle insertion in a breast is shown in Fig. 2.

The 2-D plane of the figure represents a horizontal plane passing through the target (the target mass in Fig. 2). In the figure, a simplified anatomy of the breast is shown. In reality, breast tissue is inhomogeneous and its biomechanical properties are nonlinear. Hence, if the tip of the needle reaches the interface between two different types of tissue, its further insertion will push the tissue, instead of piercing it, causing unwanted

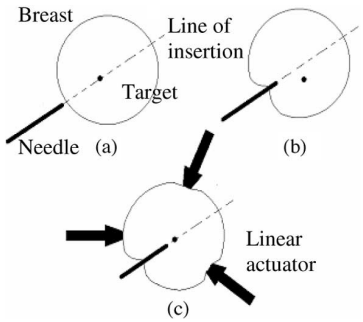

Fig. 2. Needle insertion schematic. (a) and (b) Target movement during needle insertion. (c) Minimizing needle–target misalignment using external actuators.

deformations. These deformations move the target away from its original location, as shown in Fig. 2(b). In this section, we present a controller design for the external actuators positioned around the breast, as illustrated in Fig. 2(c). These actuators apply forces on the surface of the breast based on the image of the target to guide the target toward the line of insertion of the needle.

During the biopsy procedure, the needle is inserted into the breast at a shallow angle (away from the chest wall) to the horizontal plane containing the target. The needle incision site and the orientation of the needle are chosen by the clinician, considering factors such as location of target, location of critical anatomical structures, and ease of access to target. The desired target position is the point where the line of insertion (of the needle) intersects the plane containing the target. While one can choose any plane that contains the target and has an intersection with the line of needle insertion, we choose this plane to be the horizontal plane for simplicity. The desired target position is determined by a planner based on the actual target location and needle direction. Note that we only need to control the target position in two dimensions (horizontal plane) to be able to successfully position the target along the line of insertion of the needle. Our goal is to design a controller that acts on the position error to guide the target toward the desired location. The controller is designed such that the effect of needle force (disturbance) on target position is minimized.

Before we discuss the design of the control system, we present a result from [23] to determine the number of actuators required to position the target at an arbitrary location in the horizontal plane. The following definitions are given according to the convention in [23].

Manipulation points: These are defined as the points that can be manipulated directly by robotic fingers. In our case, the manipulation points are the points where the external manipulators apply forces on the breast.

Positioned points: These are defined as the points that should be positioned indirectly by controlling manipulation points appropriately. In our case, the target is the positioned point.

The control law to be designed is noncollocated since sensor feedback is from the positioned points and control force is applied at the manipulation points. The following result is useful in determining the number of actuators required to accurately position the target at the desired location.

Result [23]: The number of manipulated points must be greater than or equal to that of the positioned points in order to realize any arbitrary displacement.

In our case, the number of positioned points is one since we are trying to control the position of just the target. Hence, ideally, the number of contact points would also be one. But practically, there are two constraints: 1) we do not want to apply shear force on the breast to avoid damage to the skin and 2) we can apply only control forces directed into the breast. We cannot pull the skin on the breast since the actuator is not attached to the breast. Thus, our problem becomes more restrictive than [23] since we need to control the position of the target by applying only unidirectional compressive force.

However, there exists a theorem on force direction closure in mechanics that helps us determine the equivalent number of normal compressive forces that can replace one unconstrained force in a 2-D (horizontal) plane.

Theorem [24]: A set of wrenches *W* can generate force in any direction if and only if there exists a three-tuple of wrenches $\{w_1, w_2, w_3\}$ whose respective force directions f_1, f_2, and f_3 satisfy the following.

1) Two of the three directions f_1, f_2, and f_3 are independent.
2) A strictly positive combination of the three directions is zero

$$\alpha f_1 + \beta f_2 + \gamma f_3 = 0.$$

The ramification of this theorem for our problem is that we need three control forces distributed around the breast [as shown in Fig. 1(c)] such that the end points of their direction vectors draw a nonzero triangle that includes their common origin point. With such an arrangement, we can realize any arbitrary displacement of the target point.

We have performed extensive simulations on a discretized model of the breast using a network of nonlinear mass–spring–dampers to determine the nature of the control laws that would be appropriate for this control problem. In particular, we investigated three generic classes of controllers: adaptive controller, force feedback controller, and a proportional integral (PI) position-error-based controller. Simulation results [25] suggest that adaptive controller and force feedback controller do not provide any significant advantage over the PI controller. Hence, a PI position-error-based controller is chosen for this application since it is the cheapest and simplest controller with acceptable performance.

Fig. 3 shows the geometry of the actuators and the target in the breast. The origin of the coordinate system is located at the initial position of the target. The error vector (e) points from current target position to desired target position. The force applied by the actuators is along directions n_1, n_2, and n_3. The PI control action is given by [23]

$$v = K_P e_n + K_I \int e_n \, d\tau \tag{1}$$

$$e_n = [e_{n1} \quad e_{n2} \quad e_{n3}]^T \tag{2}$$

where $e_{ni} (i = 1, 2, 3)$ is the projection of error (e) along the actuator direction $n_i (i = 1, 2, 3)$, K_P and K_I are 3×3 diagonal

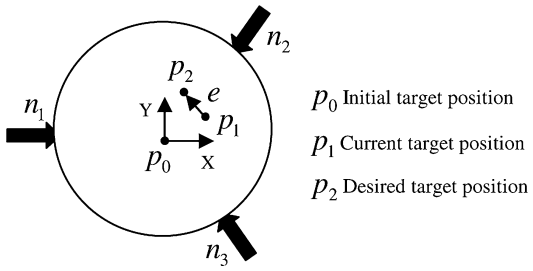

Fig. 3. Schematic of actuator and target geometry. Three external actuators are used for planar target position control.

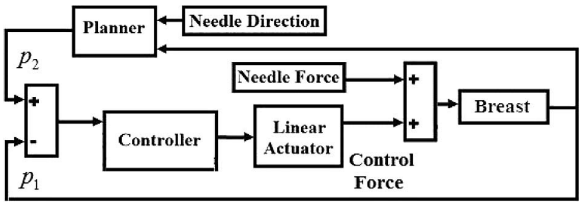

Fig. 4. Control structure for planar target position control.

matrices representing the proportional and integral gains, respectively, and v is the actuator input. Note that in control law (1), geometric or mechanical properties of the breast are not required. Fig. 4 shows a schematic of the control structure. Target position data (p_1) is obtained through image feedback. The desired target position (p_2) is determined by the planner based on the current target location and needle direction. The desired target position is always along the line of insertion of the needle. The controller acts on the position error and drives the actuators to position the target at the desired location. The force exerted by the needle is the disturbance to the system. Effect of controller windup (when tissue compression is high) can be mitigated through saturation feedback compensation [8].

In this control approach, target position is controlled in two dimensions using three actuators. In some cases, this leads to control redundancy. This redundancy is resolved by using maximum number of actuators with valid control action (control action by an actuator that results in compressive force on the breast is valid). This is achieved by defining the control error for each actuator as the projection of the error vector (e) along the direction of actuation [see (2)].

The implicit assumption in (1) is that there exists kinematic coupling between the contact points and the target. This means that applying external control force (at the contact point) in a particular direction causes the target to move in a direction that has positive projection along the direction of force. Moreover, this assumes that the internal elastic force around the target can be controlled by applying external force on the surface. This assumption is valid since breast tissue is a continuous medium, however inhomogeneous. Inhomogeneity might cause the target to deflect away from the direction of force application, but continuity of the medium ensures kinematic coupling. Weak coupling (when the target is located away from the line of action of the actuators or due to inhomogeneity in the tissue) may necessitate large external forces to position the target, but, theoretically, this does not undermine the control framework. Large external forces are undesirable so as to prevent patient injury and discomfort. This can be avoided in two ways: 1) appropriate positioning of the external actuators such that their line of action is close to the target and 2) since breast tissue is not inhomogeneous in all directions, this problem can also be obviated by distributing the actuators around the breast. The theorem and result discussed before inherently address this problem, and as an obvious consequence, the actuators are positioned 120° apart (in Fig. 3).

IV. Experimental Results

A. Phantoms

Deformable plastic phantoms with a stiff inclusion (a plastic insert placed in the phantom to mimic a tumor) are created to test the efficacy of the PI controller in positioning the inclusion at a desired location. We make the phantoms in such a manner that their material properties closely resemble breast tissue properties, as published in the literature [26]. This step is necessary to ensure the success of the presented controller when it will be applied to real breast tissue in the future. The phantom is a cylindrical structure (radius 60 mm, height 35 mm) made of polyvinyl chloride (PVC) plastic. The inclusion is a plastic sphere (radius 14 mm) that is much stiffer than the phantom. The inclusion is used as the target in the following experiments. Softening and hardening material is added to this plastic to alter its elastic property. Three phantoms (A, B, and C) are prepared with different mix ratios. Phantom A has plastic to hardener ratio of 4:1. Phantom B does not contain softener or hardener. Phantom C has plastic to softener ratio of 3:1. Procedure for preparing the phantoms is outlined in [8]. The three phantoms are homogeneous.

Uniaxial compression tests are performed on each of the phantoms to determine their elastic properties. Nominal stress–strain values are computed from force–displacement data measured during the compression test. Elastic moduli of the phantoms are determined by an exponential fit of the stress–strain curve [26]. Using the notation in [26], the stress–strain relationship is given by

$$\sigma_n^* = \frac{b^*}{m^*}(e^{m^*\varepsilon_n} - 1) \tag{3}$$

where σ_n^* is the nominal stress, ε_n is the nominal strain, and b^* and m^* are the exponential fit parameters. The Young's modulus is given by

$$E = b^* e^{m^*\varepsilon_n}. \tag{4}$$

Fig. 5 shows a plot of the Young's moduli of the phantoms. Fat tissue data shown in Fig. 5 were presented by Wellman [26]. From the figure, we can see that the phantoms have Young's moduli similar to that of a fat tissue in the breast. Breast tissue properties vary greatly based on factors such as age, presence of tissue abnormality, etc. In order to demonstrate feasibility of our technique under significant parameter variation, we prepared phantoms with varying elastic properties to demonstrate that the presented controller can work in realistic scenarios.

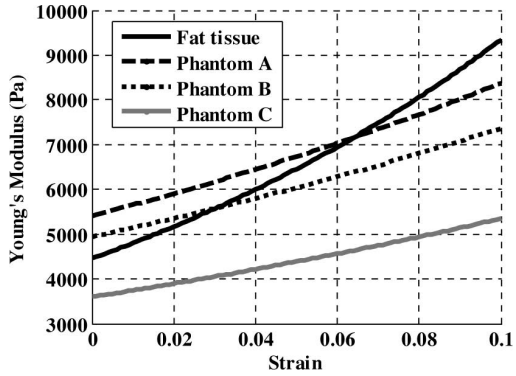

Fig. 5. Comparison of Young's modulus of fat tissue and phantoms.

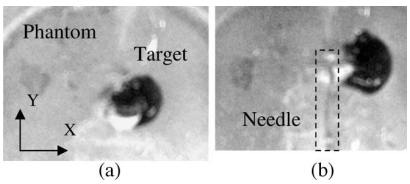

Fig. 6. Images grabbed from the video signal during needle insertion in inhomogeneous phantom. (a) Initial position of target in phantom. (b) Displacement of target from needle path. Needle is identified in the figure with a dotted bounding box.

B. Experimental Results

We demonstrate the efficacy of our technique through planar manipulation experiments. In our experiments, needle is inserted in the plane of target manipulation. Therefore, we need only two control forces (actuators) to position the target in-line with the needle. When the needle is inclined to the plane of target manipulation, we will need three control forces (actuators) to position the target on the needle path. This is because when the needle is in the plane of target manipulation, the intersection between the axis of the needle and the plane is a line, whereas when the needle is inclined to the plane, the intersection between the axis of the needle and the plane is a point. As discussed in Section III, in either case, planar manipulation is sufficient to position the target in-line with the needle. Hence, results presented in this paper also demonstrate feasibility for out-of-plane needle insertion since, in either case, we are manipulating target position in the plane.

We have performed four different experiments to demonstrate different aspects of target localization. The needle used in the following experiments is a ten-gauge vacuum-assisted device.

Experiment 1: In the first experiment, we demonstrate movement of the target during planar needle insertion. The phantoms used for this experiment are inhomogeneous (as is actual breast tissue) such that during needle insertion, the target deflects away from the path of the needle. Fig. 6 shows two images grabbed from the video signal during needle insertion. Fig. 6(a) shows the initial target location prior to needle insertion. Fig. 6(b) shows needle inserted along *Y*-axis. As the needle is inserted, the target deflects away from the needle path.

Fig. 7 shows a scatter plot of the maximum deflection of the target away from the needle path during multiple trials using

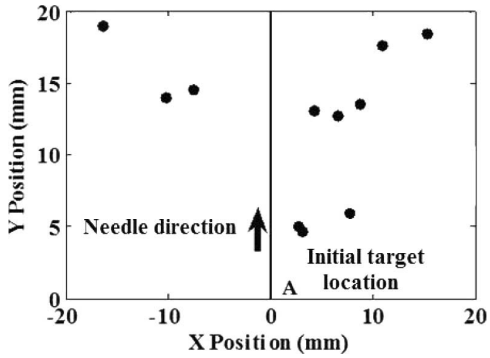

Fig. 7. Movement of target during needle insertion. Needle is inserted along *Y*-axis. Dots indicate maximum displacement of target from the needle path.

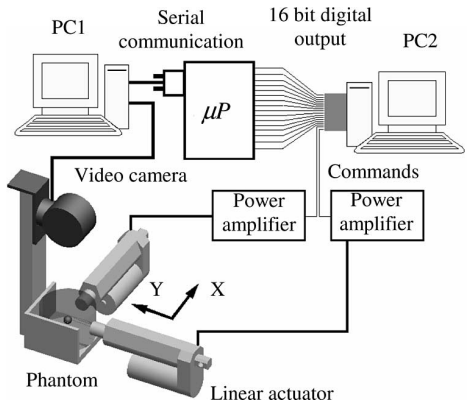

Fig. 8. Experimental setup shows system architecture and the location of actuators for target position control.

different phantoms. Point A (origin) is the initial location of the target before the needle is inserted. The arrow indicates the direction of needle insertion. During 11 trials, the average maximum deflection of the target away from the needle path is 8.51 mm. The cone angle for target deflection ranges from 28.8° to 52.3°. These results are similar to what is observed in [3]. Thus, this experiment demonstrates that the phantoms that we have created behave similar to breast tissue.

Experiment 2: An experimental setup is constructed to test the efficacy of PI-controlled linear actuators in positioning the stiff target at a desired location by applying force on the surface of the phantom. A schematic of the experimental setup is shown in Fig. 8.

The phantom is braced against a support on two sides and linear actuators apply force from the opposite sides. Position feedback is obtained using a Creative Labs video camera (30 frames per second, 640 × 480 pixels). The target can be viewed using a video camera since the phantom is transparent. Image data from the video camera are converted from red blue green (RGB) to YC_BC_R color space. The phantom is placed against a red background and the target is blue in color. Hence, chrominance (C_B) is used to track the target in real time. The image processing algorithm consists of the following steps: 1) region segmentation to extract the region of interest; 2) color space conversion to convert from RGB to YC_BC_R; 3) thresholding to differentiate the target from the background; 4) median filtering

to remove noise; and 5) blob analysis to extract target centroid coordinates.

During a biopsy procedure, image data would be obtained through US imaging. The image frames from the video camera are sent to a computer (1.6 GHz and 2 GB RAM, shown as PC1 in Fig. 8) running image processing algorithm in MATLAB. Image frames are processed to extract position data of the target. Target position data are communicated serially to a microcontroller (Freescale 68HC912B32, 8 MHz clock frequency). The microcontroller outputs these data in a 16-bit parallel format. Each iteration of image processing and data communication requires 0.2 s. This is the time delay in the feedback loop of the controller. Medical US systems have frame rates of five frames per second or higher. Hence, the time delay in the feedback loop using US systems will be the same or less and the performance of the controller will not be affected. These data are read by another computer (1.6 GHz and 1 GB RAM, shown as PC2 in Fig. 8) using a data acquisition card (Measurement Computing PCIM DDA06/16). This computer runs the PI control algorithm and outputs control signals to power amplifiers for driving the linear actuators. The linear actuators (FA-PO-20-12-2″, Firgelli Automation) are lead screw driven with inbuilt potentiometers. They have a no-load speed of 50 mm/s and a load capacity of 88 N at 25% duty cycle. The end-effector of the actuators has a circular surface area of 3.1 cm^2 (2 cm diameter). The contact between the end-effector of the actuator and phantom is frictionless.

In this experiment, we have created a situation that is similar to the target deflection problem due to a needle insertion to demonstrate the feasibility of the concept. In a needle insertion situation, the task is to localize the target so that it remains inline with the needle. Any deviation of the target is seen as an error by the controller and a compensating force is generated to mitigate the error. We assume that the target is already deflected and the task of the controller is to move the target to a desired position by applying an external force. Thus, this experiment is conducted to move the target to a desired location within the phantom using linear actuators. The initial position of the target is set as the origin. Needle force acting as a disturbance on the system is not included for this experiment. This experiment is designed to move the target along two directions (*X*- and *Y*-axes, as shown in Fig. 8) using two linear actuators perpendicular to each other. The goal is to be able to position the target at any point in the horizontal plane (*XY* plane in Fig. 8). The phantom is braced against a support opposite to the linear actuators.

In (1), duty cycle of a pulsewidth modulation (PWM) signal is used as actuator input. This is chosen to overcome friction-based limit cycle behavior seen in dc-voltage-controlled actuators. We use a PWM signal with frequency of 4 Hz and amplitude of 2 V for driving the linear actuators. The desired position of the target is 3 mm along *X*-axis and 4.2 mm along *Y*-axis. Two trials are performed with different sets of proportional and integral gains. For trial 1, proportional and integral gains are 0.02 and 0.01, respectively, for both the actuators. For trial 2, proportional and integral gains are 0.015 and 0.015, respectively, for the first actuator (acting along *X*-direction); proportional and integral gains are 0.025 and 0.015, respectively, for the second actuator

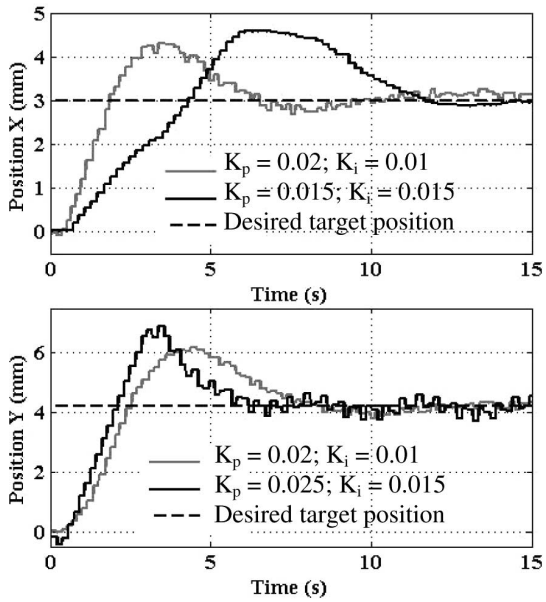

Fig. 9. Target positioning in horizontal plane. Position response of the target for two trials with different control gains. Target reaches the desired position in approximately 12 s with $K_p = 0.02$ and $K_i = 0.01$.

(acting along *Y*-direction). It can be observed from Fig. 9 that the position response for trial 1 has less overshoot along both directions. For *X*-direction, target reaches the desired position faster for trial 1. For *Y*-direction, target response has less oscillation for trial 1. Therefore, gains selected for trial 1 are better suited for target position control. It can be observed from Fig. 9 that the target reaches the desired position in approximately 12 s for trial 1. Note that any geometric or mechanical properties of the phantom are not used in the control scheme.

Experiment 3: For the third experiment, we use linear actuators to position the target during a needle insertion task. The experimental setup for this task is shown in Fig. 10.

The target is initially located at the origin and the needle is inserted along the *Y*-axis. Due to inhomogeneity in the phantom, the target moves away from the needle path during insertion. We use linear actuators positioned along the *X*-axis to steer the target toward the needle path (*Y*-axis). During this experiment, the force applied by the needle on the phantom is treated as a disturbance to the system. The task of the controller is to position the target on the *Y*-axis. The position of the target along the *Y*-axis is not controlled since the needle will intersect with the target, no matter where it is located on the *Y*-axis.

Fig. 11 shows a plot of the position response of the target (along the *X*-axis) during five trials (shown as trials 1, 2, 3, 4, and 5) on three different inhomogeneous phantoms. The inhomogeneous phantoms are constructed by distributing the phantom material A, B, and C (described in Section IV-A) in an asymmetrical arrangement during the molding process. These phantoms have two kinds of material with elastic moduli similar to fat and glandular tissue. From Fig. 11, we can see that the target is initially located on the *Y*-axis (displacement along *X*-axis is zero). As the needle is inserted, the target moves away from the *Y*-axis (nonzero displacement along *X*-axis). This initiates a

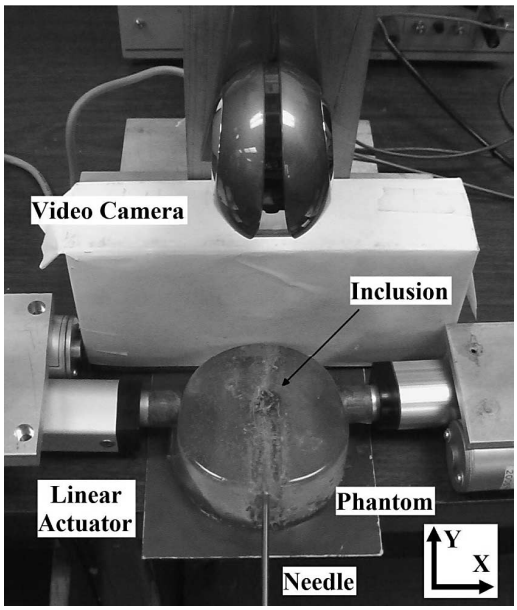

Fig. 10. Experimental setup for needle insertion task. Needle is inserted along *Y*-axis. Actuators control target position along *X*-axis.

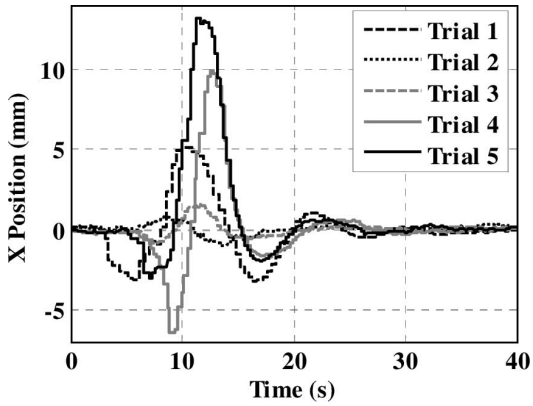

Fig. 11. Target position response during needle insertion. Plot shows that the target reaches the needle path in approximately 28 s.

control action by the actuators that steer and position the target on the *Y*-axis (displacement along *X*-axis is zero) at steady state. As we can see from Fig. 11, the target is steered back to the needle path in about 30 s. In all five trials, we were successful in positioning the target along the needle path. We could steer the target back to the needle path even when the deviation of the target is large (∼10 mm).

Fig. 12 shows the locus of the target position for trial 1. We can see from Fig. 12 that the target is initially located in the path of the needle (point A), but as the needle is inserted, it deviates away from the path and the PI-controlled actuators steer it back toward the line of insertion. The final location of the target is at point B on the needle path.

Root mean square error (RMSE) is used to quantify the targeting accuracy of this technique. RMSE is defined as

$$\text{RMSE} = \sqrt{\frac{\sum_{t=t_i}^{t_f} (x_d - x)^2}{n}} \tag{5}$$

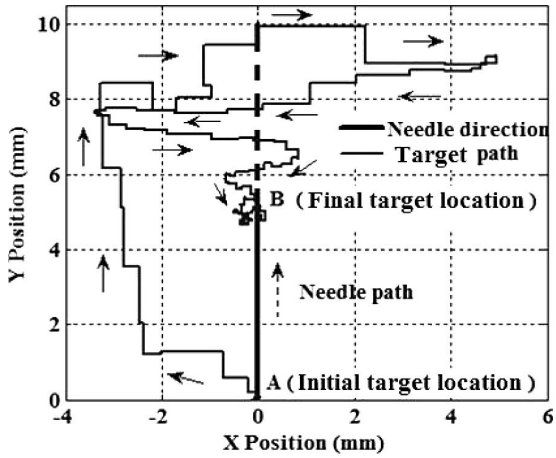

Fig. 12. Locus of target position for trial 1. Needle is inserted along the *Y*-axis. Point A is the initial target location and point B is the final target location.

TABLE I
TARGETING ACCURACY WITH EXTERNAL MANIPULATION

Trial #	1	2	3	4	5
RMSE (mm)	0.32	0.18	0.10	0.13	0.12

where t_i and t_f represent the limits of the time interval over which RMSE is computed, x_d is the desired target position, x is the actual target position at time t, and n is the number of data points in the chosen time interval. Table I shows the RMSE values for the five trials in Fig. 11. In these trials, the desired target position is along the *Y*-axis; hence, $x_d = 0$. Targeting accuracy needs to be evaluated when the target is positioned on the needle path; therefore, steady-state position data ($t_i = 30$ s; $t_f = 40$ s) are used to compute RMSE. The sampling time for the controller is 0.001 s; hence, $n = 10\,001$. As we can see from Table I, the targeting error in all cases is one order of magnitude less than the diameter of the needle (ten guage, 3.4 mm). Therefore, this technique can be used to successfully position the target on the needle path.

Experiment 4: We present preliminary results with a 2-D US system to demonstrate applicability of this technique using US image feedback. The experimental setup is shown in Fig. 13. Image feedback is obtained using a Toshiba ECCO-CEE (model SSA-340A) US system. US images are acquired using a frame grabber card (Data Translation, DT3120). Fig. 14 shows an image grabbed from the video signal of the US system. Dark blob in the image is the target. Region segmentation, thresholding, median filtering, and blob analysis are used to extract target position coordinates.

The task description for this experiment is similar to *experiment 3.* The target is initially located at the origin and the needle is inserted along the *Y*-axis (see Fig. 13). We use linear actuators positioned along the *X*-axis to steer the target toward the needle path (*Y*-axis). The task of the controller is to position the target on the *Y*-axis. *XY* plane is the imaging plane of the US probe. In this setup, positions of the actuators and needle (with respect to the US image space) are hard-coded into controller.

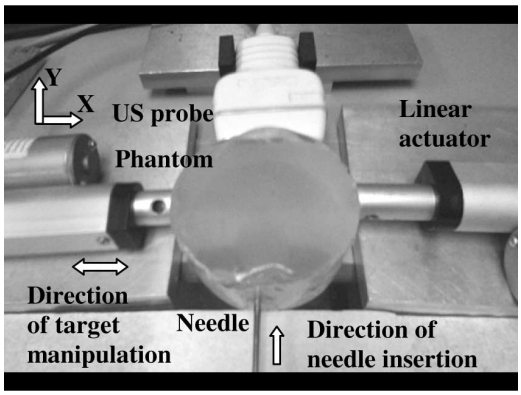

Fig. 13. US experimental setup. Needle is inserted along *Y*-axis and actuators control target position along *X*-axis.

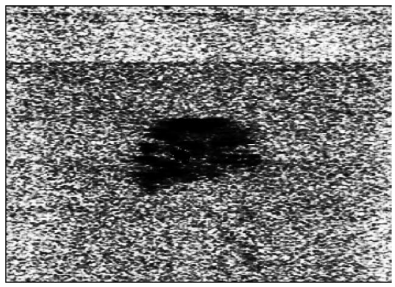

Fig. 14. US image of target in phantom. Dark blob in the image is the target.

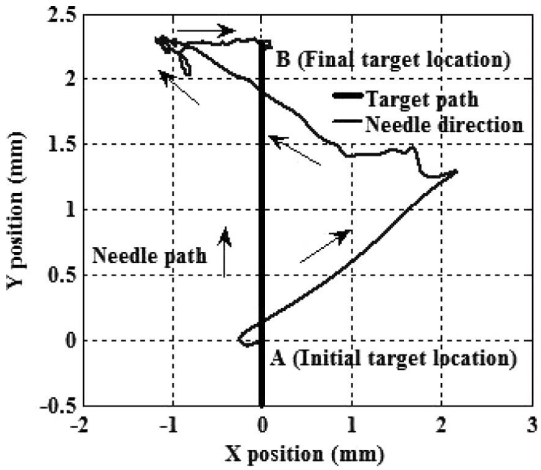

Fig. 15. Locus of target position for *experiment 4*. Needle is inserted along the *Y*-axis. Point A is the initial target location and point B is the final target location.

Fig. 15 shows the locus of target position. We can see from Fig. 15 that the target is initially located in the path of the needle (point A), but as the needle is inserted, it deviates away from the path and the actuators steer it back toward the line of insertion. The final location of the target is at point B on the needle path where it meets the needle. RMSE in this experiment is 0.06 mm.

During needle insertion, real-time video (rendered on US or computer monitor display) provides visual information of the position of the needle and target. In these experiments, operator controls needle insertion depth based on visual feedback so that the needle does not overshoot/cross the target location. If needle insertion is automated, target manipulation has to be coordinated with needle insertion so as to ensure alignment of the target with needle tip.

V. Conclusion

We have presented a new paradigm of target manipulation that uses externally controlled actuators to position a target in-line with the surgical instrument during minimally invasive procedures. Even though this approach is motivated by its application to breast biopsy, it could potentially be used for target localization during ablation, cryotherapy, etc.

PI control architecture has been presented in the paper for guiding the target toward the line of insertion of a needle. The performance of the controller is tested on phantoms with elastic property similar to that of breast tissue. We have demonstrated planar needle insertion as a proof-of-concept of a new control approach to target manipulation. As discussed in Section IV-B, it does not limit the scope of our results. Results show that PI-controlled actuators can be used to efficiently position a target in-line with needle during insertion. The proposed technique of guiding breast biopsy can increase the success rate of the procedure and enhance diagnostic outcome by reducing false negative results. The entire procedure is predicted to be fast, making it clinically viable. Since the needle is not steered inside the breast, tissue damage is also minimized. Additionally, since multiple insertions are not required, the proposed technique will likely reduce clinician fatigue and patient discomfort, and improve the structural integrity of the tissue specimen. Geometric and mechanical properties of the breast are not required for precise positioning of the target.

Target identification in US is a significant challenge, and as such, our study does not address this issue. The targets in our experiments are easily identifiable in the video frame. There exists literature on robot control using US image feedback (see, for instance, [27]). The focus of this paper is on developing a new targeting approach for needle biopsy procedures that can be integrated with any real-time imaging modality.

The proposed technique is not without limitations. In the experimental setup, position of the needle (with respect to the image space) is hard-coded into the controller. However, this would be infeasible in a clinical setting. Therefore, needle position/orientation has to be measured using a 6-DOF electromagnetic sensor, or estimated using needle segmentation techniques in US image.

The end-effector of the actuator has a circular cross section with 20 mm diameter. During experimental tests, we observed that maximum target movement in any direction is typically in the range of 5–10 mm. Since the end-effector has surface contact (contact are 3.14 cm^2), even if the target moves out of plane, the actuators can still control the target motion without causing instability. It is highly unlikely that target movement will be greater than 20 mm. If such an extreme case is observed, the robotic system requires another DOF so that the actuators can move in a direction perpendicular to the plane of manipulation. However, issues relating to stability for out-of-plane target movements have not been investigated in this paper.

Real-time automated target tracking using US is a challenging task, especially since US gives image of a 2-D cross section. To overcome this, we are currently working on designing a target tracking system for tracking out-of-plane target movement. This system continuously orients the transducer such that the 3-D coordinates of the target are tracked in real time. The target manipulation technique presented in this paper will be integrated with the target tracking system to provide comprehensive robot assistance during US-guided needle breast biopsy procedures.

REFERENCES

[1] American Cancer Society. (2008, May 16). Cancer facts & figures—2008 [Online]. Available: http://www.cancer.org/downloads/STT/2008CAFFfinalsecured.pdf

[2] J. G. Elmore, K. Armstrong, C. D. Lehman, and S. W. Fletcher, "Screening for breast cancer," *J. Amer. Med. Assoc.*, vol. 293, no. 10, pp. 1245–1256, Mar. 2005.

[3] S. P. DiMaio and S. E. Salcudean, "Needle insertion modeling and simulation," *IEEE Trans. Robot Autom.*, vol. 19, no. 5, pp. 864–875, Oct. 2003.

[4] L. Liberman, T. L. Feng, D. D. Dershaw, E. A. Morris, and A. F. Abramson, "US-guided core breast biopsy: Use and cost-effectiveness," *Radiology*, vol. 208, pp. 717–723, 1998.

[5] B. D. Fornage, "Sonographically guided needle biopsy of nonpalpable breast lesions," *J. Clin. Ultrasound*, vol. 27, no. 7, pp. 385–389, Sep. 1999.

[6] T. A. S. Matalon and B. Silver, "US guidance of interventional procedures," *Radiology*, vol. 174, pp. 43–47, 1990.

[7] W. L. Smith, K. J. M. Surry, G. R. Mills, D. B. Downy, and A. Fenster, "Three-dimensional ultrasound-guided core needle breast biopsy," *Ultrasound Med. Biol.*, vol. 27, no. 8, pp. 1025–1034, 2001.

[8] V. Mallapragada, N. Sarkar, and T. Podder, "A robotic system for real-time tumor manipulation during image guided breast biopsy," in *Proc. IEEE Int. Conf. Bioinf. Bioeng.*, Oct. 2007, pp. 204–210.

[9] V. Mallapragada, N. Sarkar, and T. Podder, "Robot assisted real-time tumor manipulation for breast biopsy," in *Proc. IEEE Int. Conf. Robot. Autom.*, May 2008, pp. 2515–2520.

[10] K. Cleary, A. Melzer, V. Watson, G. Kronreif, and D. Stoianovici, "Interventional robotic systems: Applications and technology state-of-the-art," *Minim. Invasive Ther. Allied Technol.*, vol. 15, no. 2, pp. 101–113, 2006.

[11] N. V. Tsekos, J. Shudy, E. Yacoub, P. V. Tsekos, and I. G. Koutlas, "Development of a robotic device for MRI-guided interventions in the breast," in *Proc. Bioinf. Bioeng. Conf.*, 2001, pp. 201–208.

[12] D. Stoianovici, L. Whitcomb, J. Anderson, R. Taylor, and L. Kavoussi, "A modular surgical robotic system for image guided percutaneous procedures," in *Proc. MICCAI*, 1998, vol. 1496, pp. 404–410.

[13] K. Cleary, M. Freedman, M. Clifford, D. Lindisch, S. Onda, and L. Jiang, "Image-guided robotic delivery system for precise placement of therputic agents," *J. Control. Release*, vol. 74, no. 1, pp. 363–368, Jul. 2001.

[14] A. Patriciu, S. Solomon, L. Kavoussi, and D. Stoianovici, "Robotic kidney and spine percutaneous procedures using a new laser-based CT registration method," in *Proc. MICCAI*, 2001, vol. 2208, pp. 249–257.

[15] D. Stoianovici, J. A. Cadeddu, R. D. Demaree, S. A. Basile, R. H. Taylor, L. L. Whitcomb, W. N. Sharpe, Jr., and L. R. Kavoussi, "A novel mechanical transmission applied to percutaneous renal access," in *Proc. ASME Dyn. Syst. Control Div. (DSC)*, vol. 61, pp. 285–296, Jun. 2005.

[16] S. Okazawa, R. Ebrahimi, J. Chuang, S. E. Salcudean, and R. Rohling, "Hand-held steerable needle device," *IEEE/ASME Trans. Mechatronics*, vol. 10, pp. 285–296, Jun. 2005.

[17] D. Glozman and M. Shoham, "Image-guided robotic flexible needle steering," *IEEE Trans. Robot.*, vol. 23, no. 3, pp. 459–467, Jun. 2007.

[18] R. J. Webster III, J. S. Kim, N. J. Cowan, G. Chirikjian, and A. M. Okamura, "Nonholonomic modeling of needle steering," *Int. J. Robot. Res.*, vol. 25, no. 5/6, pp. 509–526, May/Jun. 2006.

[19] P. Sears and P. Dupont, "A steerable needle technology using curved concentric tubes," in *Proc. IEEE/RSJ Int. Conf. Intell. Robots Syst.*, Oct. 2006, pp. 2850–2856.

[20] M. H. Loser and N. Navab, "A new robotic system for visually controlled percutaneous interventions under CT fluoroscopy," in *Proc. MICCAI*, 2000, vol. 1935, pp. 887–896.

[21] F. S. Azar, D. N. Metaxas, and M. D. Schnall, "Methods for modeling and predicting mechanical deformations of the breast under external perturbations," *Med. Image Anal.*, vol. 6, pp. 1–27, 2002.

[22] R. Alterovitz, K. Goldberg, J. Pouliot, R. Taschereau, and I.-C. Hsu, "Sensorless planning for medical needle insertion procedures," in *Proc. IEEE Int. Conf. Intell. Robots Syst.*, Oct. 2003, pp. 3337–3343.

[23] T. Wada, S. Hirai, S. Kawamura, and N. Kamiji, "Robust manipulation of deformable objects by a simple PID feedback," in *Proc. Int. Conf. Robot. Autom.*, 2001, pp. 85–90.

[24] V. D. Nguyen, "Constructing force-closure grasps," in *Proc. Int. Conf. Robot. Autom.*, vol. 3, pp. 1368–1373, 1986.

[25] V. Mallapragada, "Control strategies for target manipulation in deformable objects," Robot. Auton. Syst. Lab., Dept. Mech. Eng., Vanderbilt Univ., Nashville, TN, Tech. Rep., 2007.

[26] P. Wellman, "Tactile imaging," Ph.D. dissertation, Div. Eng. Appl. Sci., Harvard Univ., Cambridge, MA, 1999.

[27] P. Abolmaesumi, S. E. Salcudean, W. Zhu, M. R. Sirouspour, and S. P. DiMaio, "Image-guided control of a robot for medical ultrasound," *IEEE Trans. Robot. Autom.*, vol. 18, no. 1, pp. 11–23, Feb. 2002.

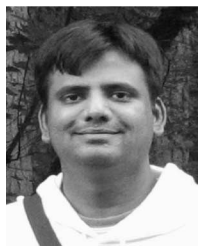

Vishnu G. Mallapragada received the B.Tech. degree in mechanical engineering from the Indian Institute of Technology, Chennai, India, in 2002, and the M.S. degree in mechanical engineering from North Carolina State University, Raleigh, in 2004. He is currently working toward the Ph.D. degree in the Mechanical Engineering Department, Vanderbilt University, Nashville, TN.

His current research interests include biomedical robotics, mechatronics, and control systems.

Nilanjan Sarkar (M'93–SM'04) received the Ph.D. degree in mechanical engineering and applied mechanics from the University of Pennsylvania, Philadelphia.

He was a Postdoctoral Fellow at Queen's University, Canada. He was also an Assistant Professor at the University of Hawaii. He is currently an Associate Professor in the Mechanical Engineering Department and the Computer Engineering Department, Vanderbilt University, Nashville, TN. His current research interests include robotics, control, and human–robot interaction.

Dr. Sarkar was an Associate Editor for the IEEE TRANSACTIONS ON ROBOTICS.

Tarun K. Podder (S'98–00–M'01) received the M.E. degree in mechanical engineering from the Indian Institute of Science, Bengaluru, India, in 1990, and the Ph.D. degree in robotics and automation from the University of Hawaii at Manoa, Honolulu, in 2000.

From 1990 to 1991, he was a Research Engineer at the Robotics and Mechatronics Centre, Indian Institute of Technology (IIT), Kanpur, India. From 1991 to 1997, he was a Lecturer in the Department of Mechanical Engineering, University of Calcutta. From 2001 to 2006, he was with Rochester Institute of Technology (RIT), RSystems, Inc., the Monterey Bay Aquarium Research Institute (MBARI), and the University of Rochester as a Research Scientist, a Research Specialist and a Project Manager, a Research Fellow, and a Research Assistant Professor, respectively. He is currently an Assistant Professor in the Department of Radiation Oncology, Thomas Jefferson University Hospital, Philadelphia, PA. His current research interests include system dynamics, path planning and control of robotic and autonomous systems, medical robotics, and robot-assisted radiation therapy.

Dr. Podder is a member of the American Society of Mechanical Engineers (ASME), the Engineering in Medicine and Biology Society (EMBS), the Robotics and Automation Society (RAS), the American Association of Physicists in Medicine (AAPM), and the American Society for Therapeutic Radiology and Oncology (ASTRO).